

## New Structural Elements in Ternary Carbides

Bambar Davaasuren, Horst Borrmann, Enkhtsetseg Dashjav, Guido Kreiner, Walter Schnelle, Frank R. Wagner, and Rüdiger Kniep

### Introduction

A few years ago we introduced the concept of carbometalates [1] which was then successfully applied to a number of novel low-valency carbomolybdates  $RE_2[MoC_2]$  ( $RE = Pr, Nd$ ),  $RE_2[Mo_2C_3]$  ( $RE = Ce, Pr, Sm, Gd - Dy$ ), -tungstates  $RE_2[WC_2]$  ( $RE = Ce - Nd$ ), and the -chromate  $Sm_2[Cr_2C_3]$  [2-6]. Recently, we focused our research on rare-earth carboferrates  $RE_xFe_yC_z$ . Out of these ternary systems only a small number of intermediate phases along with their crystal structures are reported so far ( $RE_2FeC_4$ :  $RE = Y, Tb - Lu$  [7];  $Sc_3FeC_4$  [8];  $REFeC_2$ :  $RE = Sc, Sm, Gd - Er, Lu$  [9,10]; and  $RE_{3,67}FeC_6$ :  $RE = La - Nd, Sm$  [11,12]). These crystal structures, however, contain diatomic  $C_2$ -species instead of monoatomic carbo-ligands. Further reports deal with ternary phases of approximate compositions  $GdFeC$ ,  $RE_2Fe_2C_3$  and  $RE_4Fe_4C_7$  ( $RE = Ce, Gd$ ) [13,14], the crystal structures of which remain unresolved.

Here, we report on the new rare-earth iron carbides  $RE_{15}Fe_8C_{26}$  ( $RE = Y, Dy - Er$ ) [15] and  $RE_{5,67}Fe_2C_9$  ( $RE = Y, Gd - Dy$ ) [16]. Again, these compounds do not represent pure carbometalates as their crystal structures contain diatomic  $C_2$  units besides monoatomic C species. Crystal structures, chemical bonding analyses and physical properties are presented along with first perspectives towards an extension of the carbometalates concept.

The new compounds were prepared by arc-melting of cold-pressed pellets of mixtures of rare-earth and iron metals together with graphitic carbon. The samples were annealed at 1173 K and 1373 K in arc-welded Ta ampoules encapsulated in evacuated and fused silica tubes for 7 to 30 days. The dark grey reaction products with metallic luster are sensitive to air and moisture. Accordingly, all handlings were performed in protective Ar atmosphere. For characterization, X-ray diffraction techniques, metallographic examinations combined with WDXS, and measurements of magnetic susceptibility and electrical resistivity were applied.

### $Dy_{15}Fe_8C_{26}$ : a new structure type containing $Fe_6$ clusters

The isotopic series of  $RE_{15}Fe_8C_{26}$  ( $RE = Y, Dy - Er$ ) represents a new structure type. Lattice parameters (see Tab. 1) decrease from the Y to the Er-compound. Both, X-ray diffraction on powders and WDXS analyses on polished samples indicated the presence of a minor amount (<2 vol. %) of impurity phases. Ta contamination from the crucible has not been detected.

Table 1: Unit cell parameters and unit cell volumes of  $RE_{15}Fe_8C_{26}$ .

Compound	<i>a</i> (pm)	<i>c</i> (pm)	<i>V</i> (10 <sup>6</sup> pm <sup>3</sup> )
$Y_{15}Fe_8C_{26}$	1194.92(4)	513.83(3)	636.37(5)
$Dy_{15}Fe_8C_{26}$	1192.63(2)	514.36(2)	633.59(3)
$Ho_{15}Fe_8C_{26}$	1189.11(7)	511.26(5)	626.06(8)
$Er_{15}Fe_8C_{26}$	1185.29(4)	508.46(4)	618.64(1)

Here, we exemplarily report on the crystal structure of  $Dy_{15}Fe_8C_{26}$ . This structure was determined from single crystal X-ray analyses, solved by direct methods and refined in the space group  $P321$  (no. 150) to residuals of  $R1 = 0.024$  and  $wR2 = 0.053$  for 1345 unique reflections and 58 variables [17]. The specimen under investigation was a merohedral twin (twin laws:  $010\ 100\ 001$  and  $\bar{1}\ 00\ 0\bar{1}\ 0\ 00\bar{1}$ ; fractions of domains: 0.81, 0.19, 0.48, 0.17). All atomic sites were fully occupied.

The crystal structure of  $Dy_{15}Fe_8C_{26}$  can be described in terms of stacking of polyanionic slabs  ${}^z_2[Fe_8(C_2)_{12}(C)_2]^{45-}$  along [001] with the  $Dy^{3+}$  ions in between (Fig. 1). The structure contains Fe atoms at three different crystallographic sites coordinated by two different kinds of ligands, monoatomic and diatomic carbon species. As shown in Fig. 2, the coordination polyhedra around the Fe atoms are distorted tetrahedra (a)  $Fe1(C_2)_4$ , (b)  $Fe2C_2(C_2)_2$  and distorted planar trigonal units (c)  $Fe3(C_2)_3$ .

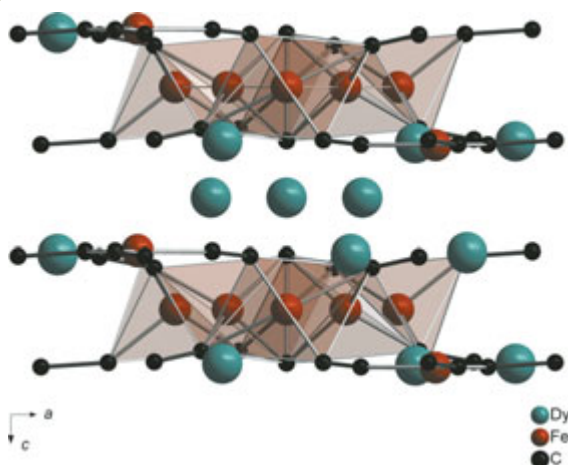


Fig. 1: The crystal structure of  $Dy_{15}Fe_8C_{26}$  viewed along the  $[010]$  direction. The polyhedra around Fe atoms are formed by monoatomic and diatomic carbon ligands.

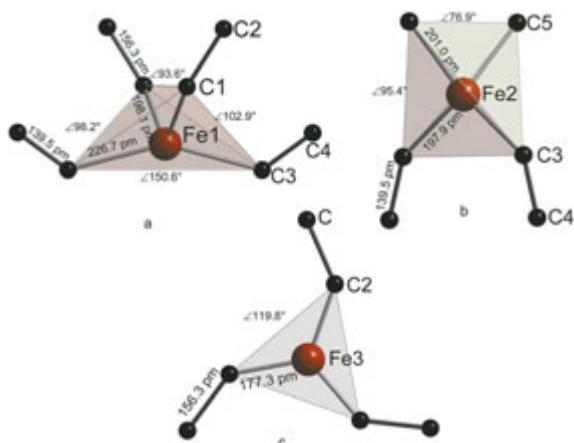


Fig. 2: Coordination polyhedra around the three crystallographically different Fe sites in the crystal structure of  $Dy_{15}Fe_8C_{26}$ .

A striking feature of this structure is a group of six Fe atoms, which are condensed into a slightly distorted triangle with Fe atoms at the vertices (Fe1) and at the midpoints of the triangular edges (Fe2) with the distances  $d(Fe2-Fe2) = 272.3$  pm and  $d(Fe1-Fe2) = 257.9$  pm (Fig. 3). The three  $Fe_2C_2(C_2)_2$  units of the inner triangle share a common edge formed by a  $C^{4-}$  ligand. These groups are further connected to neighbouring  $Fe_1(C_2)_4$  units via carbon atoms of the  $C_2$  pairs. Each  $Fe_6$  group is linked to three surrounding  $Fe_6$  groups via six trigonal planar  $Fe_3(C_2)_3$  units by sharing end-on bonded  $C_2$  ligands, thus forming infinite layers.

The distribution of the Dy atoms can be described as follows: the  $Fe_3(C_2)_3$  unit is surrounded by nine Dy atoms (Dy1, Dy2) in a tri-capped trigonal prismatic arrangement and stacked along  $[001]$

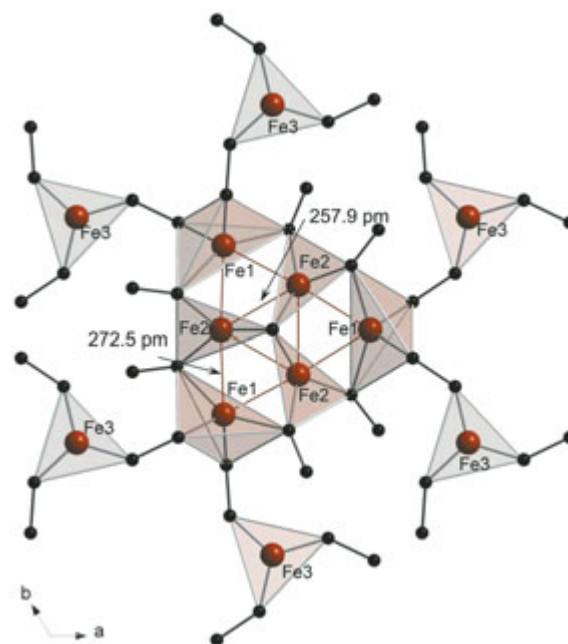


Fig. 3: Detail of the polyanionic slab  $\frac{2}{3}[Fe_8(C_2)_{12}(C_2)_2]^{45-}$  revealing the linkages of the different Fe-coordination polyhedra.

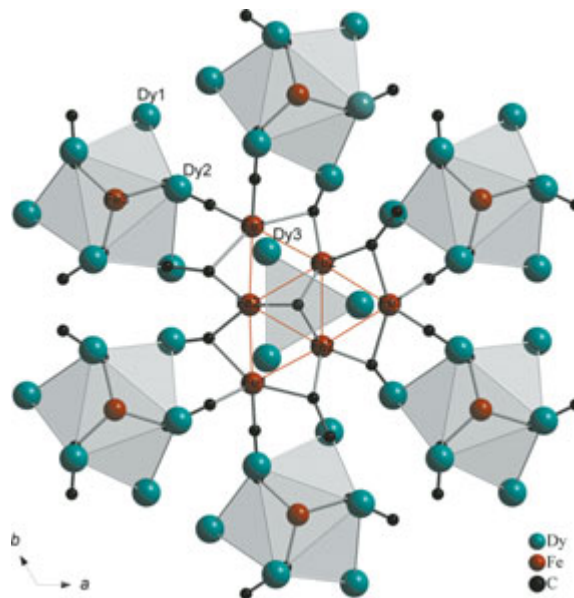


Fig. 4: The crystal structure of  $Dy_{15}Fe_8C_{26}$  viewed along  $[001]$ : infinite chains of trigonal and tricapped trigonal prismatic Dy-polyhedra can be recognized. The following distances have been determined:  $d(Fe-C) = 177.3$  pm – 226.7 pm,  $d(Dy-C) = 230.1$  pm – 277.1 pm,  $d(Dy-Fe) = 274.5$  pm – 325.2 pm,  $d(Dy-Dy) = 340.9$  pm – 396.5 pm.

by sharing common basal faces. This results in a honeycomb-like columnar arrangement of Dy polyhedra. The large prismatic channels of the honeycomb net contain the planar  $Fe_6$  groups, which are embedded in a matrix of Dy atoms. Along with the Dy3 atoms, the latter form a central column of trigonal prisms sharing common basal planes (Fig. 4).

The corrected magnetic susceptibility of  $\text{Dy}_{15}\text{Fe}_8\text{C}_{26}$  above 100 K follows a Curie-Weiss law with  $\mu_{\text{eff}} = 10.0 \mu_{\text{B}}/\text{Dy-atom}$ , which is compatible with  $\text{Dy}^{3+}$  ions and non-magnetic Fe species (Fig. 5). A broad transition at  $T \approx 16$  K in low magnetic fields (not seen in Fig. 5) indicates a complex magnetic ordering of the Dy moments. Although the electrical resistivity of a bulk sample ( $\rho_0 \approx 0.30 \text{ m}\Omega \text{ cm}$ ,  $\rho(300\text{K}) = 0.63 \text{ m}\Omega \text{ cm}$ ) is rather high it increases slightly with temperature confirming that  $\text{Dy}_{15}\text{Fe}_8\text{C}_{26}$  is a metal. XAS measurements (DESY, Hamburg) at the Fe-K edge of the Dy compound in comparison with  $\text{Er}_2\text{Fe}^{\text{II}}\text{C}_4$  [7] and Fe-powder as reference compounds suggest an oxidation state close to +2 for Fe (Fig. 6).

For  $\text{Y}_{15}\text{Fe}_8\text{C}_{26}$  the electronic structure was calculated from first principles using the self-consistent TB-LMTO-ASA method [18] within the local density approximation [19] to the density functional theory. Chemical bonding analyses were carried

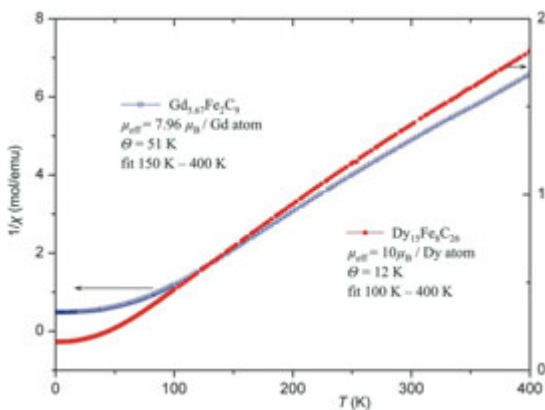


Fig. 5: Inverse magnetic susceptibility  $1/\chi = H/M$  of  $\text{Dy}_{15}\text{Fe}_8\text{C}_{26}$  and  $\text{Gd}_{5.67}\text{Fe}_2\text{C}_9$  versus temperature at an external field of  $\mu_0 H = 7 \text{ T}$ .

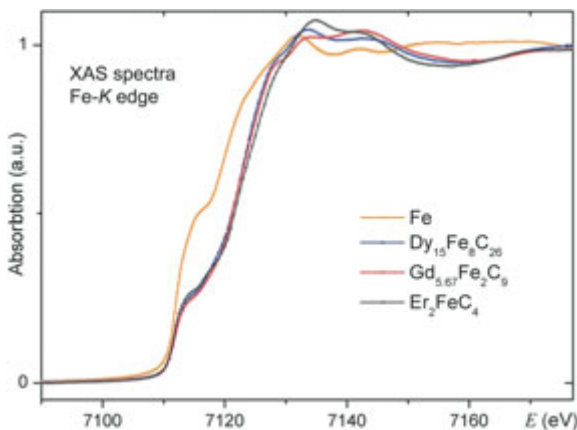


Fig. 6: XAS spectra at the Fe-K edge of  $\text{Dy}_{15}\text{Fe}_8\text{C}_{26}$  and  $\text{Gd}_{5.67}\text{Fe}_2\text{C}_9$  with references Fe and  $\text{Er}_2\text{FeC}_4$ .

out using COHP [20] and ELI-D [21,22]. The total DOS shows 173 states/eV at  $E_{\text{F}}$ , i.e., the compound is metallic. COHP calculations indicate strong covalent Fe-C and C-C bonds as well as considerable Fe-Fe interactions which are exhausted below  $E_{\text{F}}$  (Fig. 7).

The averaged ICOHP(Y-C) value yields approximately one quarter of that of the Fe-C bonds and hence, resembles the values observed in carbometalates [1]. The ratio ICOHP(Metal-Carbon)/ICOHP(Metal-Metal) amounts to 3, which is at the lower limit for polyanionic compounds as reported in [1]. The ELI-D reveals three different attractor types for the anionic part of the structure, covalent Fe-C bonds, lone pairs around the non-bonded carbon atoms of the  $\text{C}_2$  pairs and multi-center

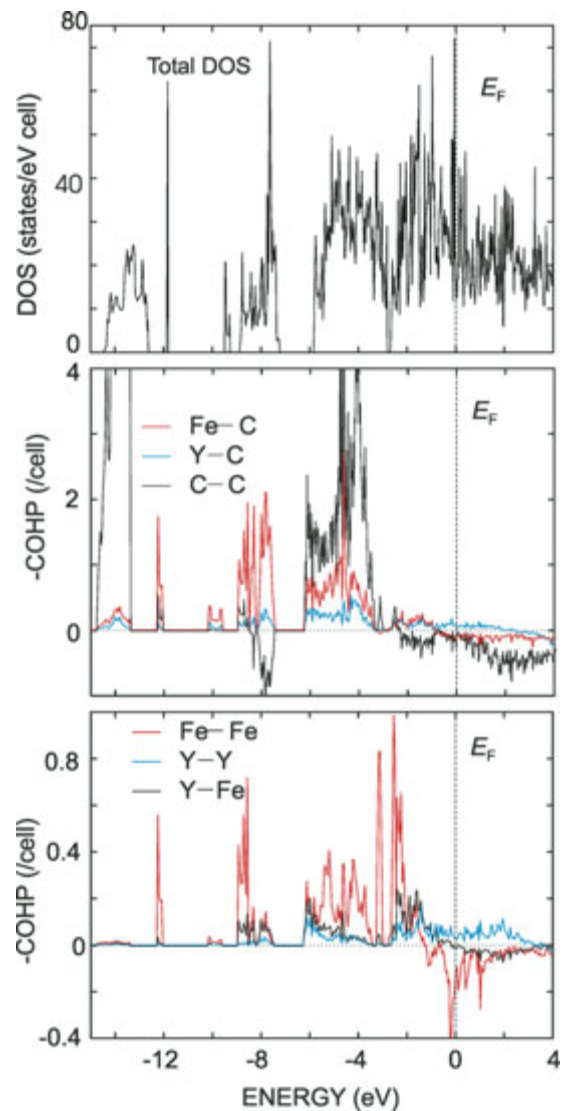


Fig. 7: Total DOS and COHP diagrams for selected interatomic interactions in the crystal structure of  $\text{Y}_{15}\text{Fe}_8\text{C}_{26}$ .

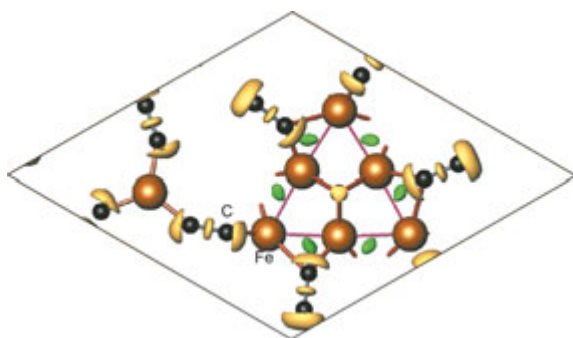


Fig. 8: ELI-D presentation for the polyanionic part of the crystal structure of  $Y_{15}Fe_8C_{26}$ : light brown domains (isovalue  $Y_D = 1.49$ ) indicate covalent bonds Fe–C and lone pairs around the free ends of  $C_2$ -pairs and monoatomic C, green domains (isovalue  $Y_D = 1.01$ ) indicate multicenter metal-metal bonds.

metal-metal bonds. The local maxima of the metal-metal bonds are clearly shifted towards the Fe–Fe bonds within the  $Fe_6$  cluster (Fig. 8).

The edge and vertex sharing  $FeC_4$  tetrahedra in the crystal structure of  $Dy_{15}Fe_8C_{26}$  resemble the anionic structural motives commonly found in the crystal structures of carbomolybdates [1]. Trigonal planar complexes are also known in carborhenates [23]. The  $C_2$  pairs serve as bridging ligands between Fe1 and Fe2 as well as between Fe1 and Fe3. In the first case one carbon atom of the  $C_2$  unit is the donor atom while the remaining one carries a lone pair. In the second case bridging is performed via both carbon atoms, i.e., one carbon serves as the donor atom towards Fe1 whereas the other one donates towards Fe3.

### $Gd_{0.67}Gd_5Fe_2C_9$ : a new structure type containing anionic complexes $\infty^0 [FeC(C_2)_2]$ and $\infty^1 [Fe(C_2)_{4/2}]$

The X-ray diffraction pattern of single crystals of  $Gd_{0.67}Gd_5Fe_2C_9$  exhibits satellite reflections. The main reflections could be indexed assuming an orthorhombic cell ( $a = 2946.8(1)$  pm,  $b = 510.4(1)$  pm,  $c = 1276.2(1)$  pm,  $V = 1919 \cdot 10^6$  pm<sup>3</sup>). The modulation vector corresponds to  $q \approx 3/2b^*$ . A preliminary structure model was obtained by direct methods using only the main reflections. Subsequently, it was refined in the space group  $Pnma$  with anisotropic displacement parameters for all atoms to residuals  $R1 = 0.048$  and  $wR2 = 0.132$  for 2776 observed unique reflections and 209 variables. The refinement reveals full occupancy for all atomic sites

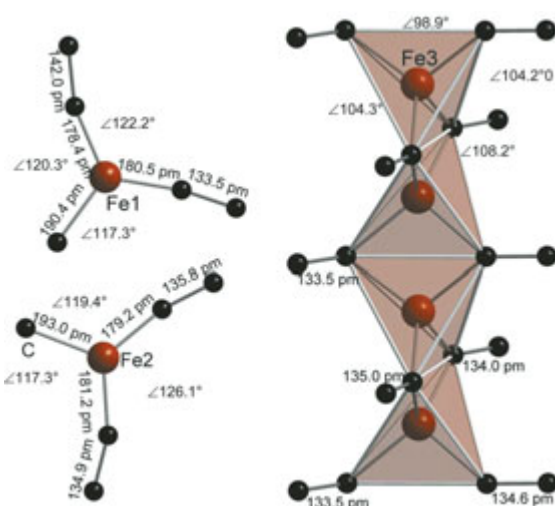


Fig. 9: Complex anions in the crystal structure of  $Gd_{0.67}Gd_5Fe_2C_9$ : coordination around Fe by C- and  $C_2$ -ligands.

except for three Gd positions (each occupied by about 20%) with very short Gd – Gd distances between 62 pm and 253 pm.

The structure contains two different anionic complexes: discrete units  $Fe1C(C_2)_2$  with distorted trigonal planar arrangement around the Fe atom and infinite tetrahedral chains of composition  $Fe2(C_2)_2$ . In the latter the  $C_2$  ligands are bonded end-on via one C as the donor atom to the central Fe atom. The resulting  $FeC_4$ -tetrahedra form chains running along [010] by sharing common edges, in analogy to the linkage principle found in the crystal structure of  $SiS_2$  (Fig. 9).

Each trigonal complex  $Fe1C(C_2)_2$  is surrounded by nine Gd atoms forming large tricapped trigonal prisms which are fused along [010] via common basal planes. The situation is similar to that found in the crystal structure of  $Dy_{15}Fe_8C_{26}$ . However, in the Gd-compound the columns of  $RE$  polyhedra running along [010] are condensed form double-chains (Fig. 10; see also Fig. 4).

The carbon atoms of the  $C_2$  pairs that are not acting as donor atoms towards Fe atoms form octahedral channels and running along [010]. The remaining Gd atoms occupy these channels. The respective split positions for a preliminary model are shown in Fig. 11a. A Rietveld refinement of the modulated structure including the satellite reflections using synchrotron powder data (ID31 at ESRF, Grenoble, France) has been attempted. The structure reveals a density modulation of the Gd atoms within the channel. In the powder refine-

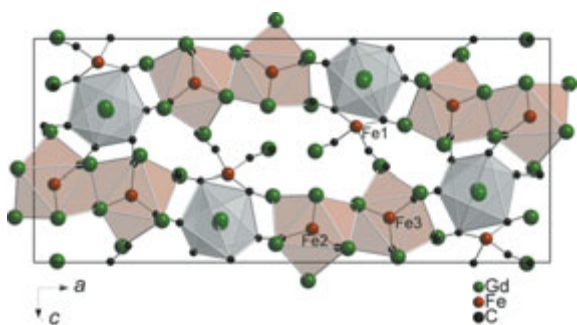


Fig. 10: The crystal structure of  $Gd_{0.67}Gd_5Fe_2C_9$  viewed along  $[010]$ . Octahedral channels (grey polyhedra, running along  $[010]$  by sharing common triangular faces) are formed by  $C_2$ -units of neighbouring complex anions: tetrahedral chains  $Fe(C_2)_{4/2}$  (ball and stick representation) and trigonal planar  $FeC(C_2)$  groups inside double chains formed from tricapped trigonal prisms of Gd (light red).

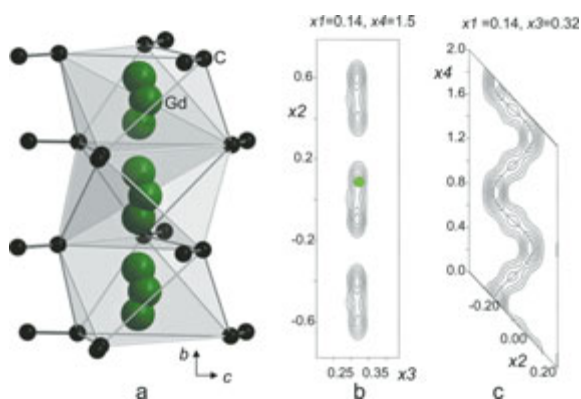


Fig. 11: a) Octahedral channel of C atoms from  $C_2$ -pairs enclosing Gd atoms in view along  $[100]$ . Their positions obtained from the single crystal structure refinement are best described by split atoms. b) Observed electron density maps of the modulated atoms from powder refinement (green dot indicates the position of modulated Gd atom) and c) modulation for these atoms.

ment the modulation vector yields  $q \approx 1.486 [010]^*$  whereas the electron density (Fig. 11b) was fitted using two parameters describing occupancy and displacement of the Gd atoms.

A more sophisticated refinement of the Gd partial structure within the octahedral channels using single crystal data is in preparation. An isotypic series  $RE_{5.67}Fe_2C_9$  ( $RE = Y, Tb, Dy$ ) of this new structure type has been prepared. The subcell parameters are listed in Table 2.

The inverse magnetic susceptibility of  $Gd_{5.67}Fe_2C_9$  displays Curie-Weiss paramagnetism with  $\mu_{\text{eff}} = 7.96\mu_B/\text{Gd-atom}$ , a value similar to that of free  $Gd^{3+}$  ions with configuration  $4f^7$  (see Fig. 5). At  $T \approx 25$  K the Gd moments order ferromag-

Table 2: Unit cell parameters and unit cell volumes of members of the isotypic series  $RE_{5.67}Fe_2C_9$ .

Compound	$a$ (pm)	$b$ (pm)	$c$ (pm)	$V$ ( $10^6 \text{pm}^3$ )
$Y_{5.67}Fe_2C_9$	2929.9(1)	502.8(3)	1260.9(5)	1857(2)
$Gd_{5.67}Fe_2C_9$	2946.8(1)	510.4(1)	1276.2(1)	1919(1)
$Tb_{5.67}Fe_2C_9$	2935.5(7)	506.1(1)	1267.5(3)	1883(1)
$Dy_{5.67}Fe_2C_9$	2929.9(2)	502.6(4)	1261.2(7)	1857(3)

netically. Electrical resistivity measurements of a bulk piece shows a decrease of  $\rho(T)$  ( $\rho_0 \approx 5.7 \text{ m}\Omega \text{ cm}$ ,  $\rho(300 \text{ K}) = 3.2 \text{ m}\Omega \text{ cm}$ ) with increasing temperature.

X-ray absorption spectra at the Fe-K threshold resemble those of  $Dy_{15}Fe_8C_{26}$  indicating an oxidation state close to +2 for Fe (see Fig. 6).

## Conclusions

The crystal structures of  $Dy_{15}Fe_8C_{26}$  and  $Gd_{0.67}Gd_5Fe_2C_9$  contain complex anions with small coordination numbers and low oxidation states of the iron atoms. The structural motives, e.g., tetrahedral and trigonal planar anionic units, in these compounds resemble those commonly found in carbometalates.  $Dy_{15}Fe_8C_{26}$  and  $Gd_{0.67}Gd_5Fe_2C_9$  are first examples of compounds in which tetrahedral and trigonal planar units coexist in one crystal structure. Though our first results on the chemical bonding in these compounds indicate a close relationship to carbometalates [1] some unique aspects arising from the presence of  $C_2$  units are of great interest and call for further detailed studies.

## References

- [1] E. Dashjav, G. Kreiner, W. Schnelle, F. R. Wagner, R. Kniep, and W. Jeitschko, *J. Solid State Chem.* **180** (2007) 636.
- [2] E. Dashjav, F. R. Wagner, W. Schnelle, G. Kreiner, and R. Kniep, *Z. Anorg. Allg. Chem.* **630** (2004) 689.
- [3] E. Dashjav, F. R. Wagner, W. Schnelle, G. Kreiner, and R. Kniep, *Z. Anorg. Allg. Chem.* **630** (2004) 2277.
- [4] E. Dashjav, F. R. Wagner, W. Schnelle, G. Kreiner, and R. Kniep, *Z. Anorg. Allg. Chem.* **633** (2007) 1349.
- [5] E. Dashjav, W. Schnelle, G. Kreiner, and R. Kniep, *Z. Kristallogr. NCS.* **220** (2005) 129.

- [6] *E. Dashjav, Yu. Prots, G. Kreiner, W. Schnelle, F. R. Wagner, and R. Kniep*, *Sc. and Technol. Adv. Mater.* **8** (2007) 364.
- [7] *M. H. Gerss, W. Jeitschko, L. Boonk, J. Nientiedt, J. Grobe, E. Mörsen, and A. Leson*, *J. Solid State Chem.* **70** (1987) 19.
- [8] *R.-D. Hoffmann, R. Pöttgen, and W. Jeitschko*, *J. Solid State Chem.* **99** (1992) 134.
- [9] *R. Pöttgen, W. Jeitschko, U. Wortmann, and M. E. Danebrock*, *J. Mater. Chem.* **2** (1992) 633–637.
- [10] *W. Jeitschko, and M. H. Gerss*, *J. Less-Common Met.* **116** (1986) 147.
- [11] *A. M. Witte, W. Jeitschko*, *Z. Naturforsch.* **51b** (1996) 249.
- [12] *B. Davaasuren, E. Dashjav, G. Kreiner, H. Borrmann, M. Mihalkovic, and R. Kniep*, 16th International Conference on Solid Comp. of Transition Elements, Dresden, Germany, 07/2008. *J. Alloys and Compd.*, in press.
- [13] *H. H. Stadelmeyer and H. K. Park*, *Z. Metallkde.* **73** (1982) 399.
- [14] *H. K. Park, H. H. Stadelmeyer, and L. T. Jordan*, *Z. Metallkde.* **72** (1981) 417.
- [15] *B. Davaasuren*, unpublished results.
- [16] *B. Davaasuren, E. Dashjav, G. Kreiner, H. Borrmann, and R. Kniep*, *Z. Anorg. Allg. Chem.* **634** (2008) 2019.
- [17] *Louis J. Farrugia*, WinGX v.1.70, An integrated System of Windows Programs for the Solution and Refinement and Analysis of Single Crystal X-ray Diffraction Data, University of Glasgow, United Kingdom, 2005.
- [18] *O. Jepsen, A. Burkhard, and O. K. Andersen*, The Program TB-LMTO-ASA, version 4.7, Max-Planck-Institut für Festkörperforschung, Stuttgart, Germany, 1999.
- [19] *U. Barth and L. Hedin*, *J. Phys.* **C5** (1972) 1629.
- [20] *R. Dronskowski, P. E. Blöchl*, *J. Phys. Chem.* **97** (1993) 8617.
- [21] *a) M. Kohout*, *Int. J. Quantum Chem.* **97** (2004) 651. 24; *b) M. Kohout*, *Faraday Discuss.* **135** (2007), 43; *c) F. R. Wagner, V. Bezugly, M. Kohout, and Yu. Grin*, *Chem. Eur. J.* **13** (2007) 5724.
- [22] *E. Dashjav, Yu. Prots, F. R. Wagner, G. Kreiner, and R. Kniep*, *J. Solid State Chem.* **181** (2008) 3121.
- [23] *M. H. Gerdes, W. Jeitschko, K.H. Wachtmann, and M. E. Danebrock*, *J. Mater. Chem.* **7** (1997) 2427.